

Research Article

Study on the Precursor Characteristics of Instability Failure of Gas-Bearing Coal Based on Stress and Gas Seepage Volume

Hui Xie,¹ Yankun Ma ,² Xiaofei Liu ,^{1,3} Jinduo Li,¹ Ang Gao,¹ and Zinan Du¹

¹School of Safety Engineering, China University of Mining and Technology, Xuzhou, Jiangsu 221116, China

²Key Laboratory of Safe and Effective Coal Mining (Anhui University of Science and Technology), Ministry of Education, Huainan, Anhui 232001, China

³Guizhou Anhe Yongzhu Technology Co., Ltd., Guiyang, Guizhou 550081, China

Correspondence should be addressed to Yankun Ma; ykma@aust.edu.cn and Xiaofei Liu; liuxiaofei@cumt.edu.cn

Received 23 April 2022; Accepted 31 May 2022; Published 25 July 2022

Academic Editor: Wen-long Shen

Copyright © 2022 Hui Xie et al. This is an open access article distributed under the Creative Commons Attribution License, which permits unrestricted use, distribution, and reproduction in any medium, provided the original work is properly cited.

In coal mining activities, the original stress of the coal body changes, resulting in structural deformation and destruction, which will cause changes in gas seepage volume. The conventional triaxial loading test was carried out by using the triaxial loading-gas adsorption seepage experimental device. The effects of different loading rates, confining pressures, and gas pressures on the peak strength of coal were analyzed; the evolution laws of coal stress, gas seepage volume, stress rate, and gas seepage volume rate at different deformation stages were studied; and it was found that the time, at which the specimen began to enter the crack propagation deformation stage, determined by the change of gas seepage rate or stress rate was not the same. Therefore, combined with gas seepage and stress, a theoretical model of stress rate-seepage volume rate under triaxial pressure was proposed, and the ratio F of the two was used as an early warning index. It was found that the F value was basically stable in the elastic stage and decreased rapidly in the crack propagation stage. Thus, the F value was used as an early warning index for the instability and failure of gas-bearing coal. The F value of the experimental results was consistent with the theoretical model, and the F value entered the crack propagation stage earlier than the stress rate or the gas seepage volume rate. The research results provided a theoretical basis for coal mine safety mining and disaster prevention.

1. Introduction

China is currently the world's largest coal producer and consumer, with coal consumption accounting for 56.0 per cent of total energy in 2018 [1], and China's coalbed methane resources ranked third globally [2]. Most of the mines that experienced disasters associated with rockburst and gas were high gas mines, in which rockburst created conditions for a large number of rapid gas emissions, and high gas pressure also constituted the dynamic conditions for rockburst [3–5]. With the gradual increase of coal mining depth, the gas pressure, gas content, and ground stress of coal seam were increasing; the gas permeability was gradually decreasing, in which the deep coal seam with high gas content gradually transformed into the outburst coal seam;

and the coal-gas dynamic disaster was becoming more and more serious [6, 7].

In recent years, many scholars have made many significant achievements in the study of coal rock gas dynamic disasters [8–11], to make people have a certain degree of understanding of the mechanism of coal rock gas dynamic disasters, in which the comprehensive action hypothesis [12, 13] indicated that the increase of gas pressure would reduce the threshold of coal strength when coal and gas outburst occurred. Former Soviet scientist Pethuoff first proposed the concept of impact-outstanding unified research. In the 1990s, according to the energy criterion, some people established the criteria for the occurrence of rockburst and coal-gas outburst disasters and proposed the unified instability theory [14], which was the first time that

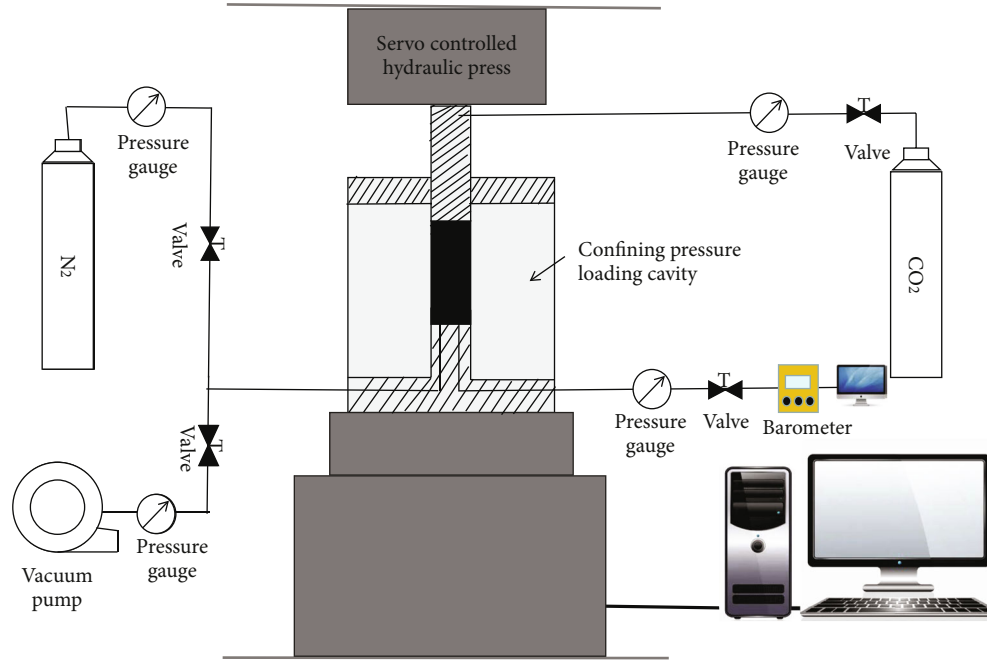


FIGURE 1: Schematic diagram of the experimental system.

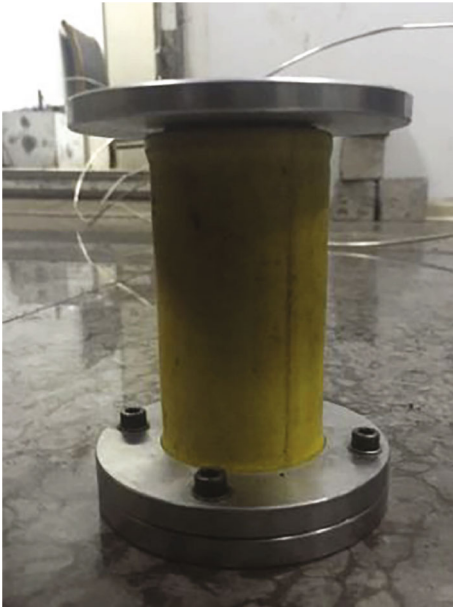


FIGURE 2: The packaged sample.

Chinese scholars had systematically explored the mechanism of coal-rock gas composite dynamic disaster. Some researchers [15] used the unified instability theory of rockburst and gas outburst to obtain the coupling relationship between the two disasters and proposed the corresponding risk assessment method. Pan [3] further divided coal dynamic disasters into four categories, coal and gas outburst, impact-gas outburst composite disaster, gas outburst-impact composite disaster, and rockburst. A compound disaster

TABLE 1: Experimental scheme.

Plan	Loading rate (mm/min)	Confining pressure (MPa)	Gas pressure (MPa)
1	0.5	0.75	0.5
2	1.0	0.75	0.5
3	1.5	0.75	0.5
4	0.5	1.5	0.5
5	0.5	2.0	0.5
6	0.5	0.75	1.0
7	0.5	0.75	1.5

model of rockburst and gas outburst in circular roadway [16] was established to study the induced transformation mechanism of rockburst and coal and gas outburst. Li et al. [17] studied the mechanical mechanism of coal and gas outburst in low-permeability outburst coal seam with soft coal seam, direct roof, and direct bottom under rockburst and proposed that the existence of hard rock in the floor should be paid attention to. In the process of deep coal seam mining, the mechanical characteristics of coal seam and gas-containing coal seam were different, because the adsorption-desorption of gas in coal was reversible, which means the adsorption of gas would cause the expansion of the coal matrix and the desorption of gas would cause the contraction of coal matrix, and these deformations changed the pore structure of coal [18, 19]. Therefore, it was of great significance to consider the influence of gas on the mechanical characteristics of coal. Many scholars proposed the constitutive equation of gas-bearing coal [20–22] and conducted experimental research. It was found that the presence of gas

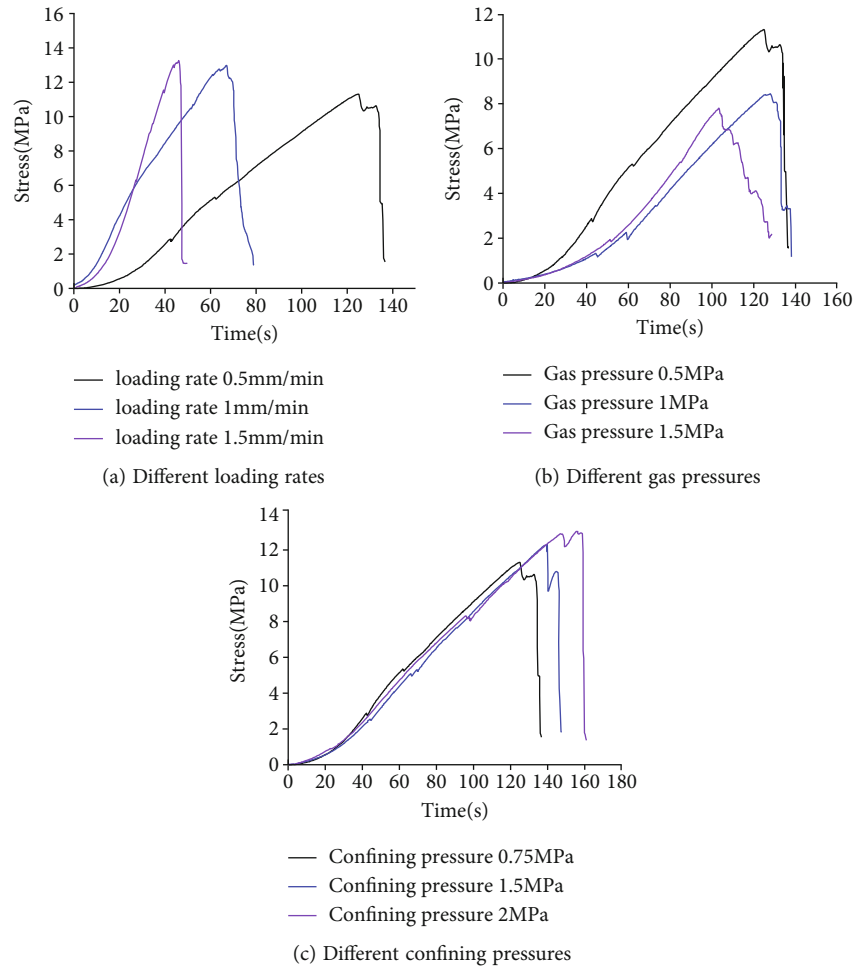


FIGURE 3: Time-axial stress curves under different loading conditions.

would reduce the strength of coal [23, 24], the elastic modulus of coal decreased with increasing gas pressure [25], the increase of gas pressure would reduce the critical shear stress of coal, and enormous initial gas pressure and low external load would cause serious coal sample damage [26]. Based on the triaxial stress loading test, the stress-strain relationship and permeability characteristics were analyzed [21, 27], and it was also concluded that the axial strain mainly occurred in the elastic deformation stage, and the failure of the sample was mainly caused by the radial strain in the elastic-plastic and plastic deformation stages [28]. With the increase of confining pressure, the peak strength of coal samples increased, and the stress drop coefficient decreased exponentially [29]. Through the true triaxial dynamic and static loading tests on gas-bearing layered composite coal and rock mass, the induced effects and dynamic behaviour characteristics of various loading factors on rockburst-outburst composite disasters were analyzed, and it was pointed out that high-pressure gas had a positive effect on the breeding of dynamic disasters [30]. Based on the mechanical test and theoretical analysis of coal samples with low gas pressure, Li and Pi believed that the coal disaster would occur in advance under the combined impact of the

roof and floor fracture [31]. These studies showed that the deformation and failure of coal were a complex evolution process, and the mechanical properties of gas-bearing coal were directly related to gas content.

The main reason for the coal and gas outburst disaster was gas seepage in the coal seam [32, 33], so domestic and foreign scholars had much research on gas permeability and achieved significant results. Wang et al. [34] studied the influence of axial stress and gas pressure on permeability. The results showed that with the increase of axial stress or gas pressure, the permeability increased, and the axial stress had a greater impact on it. The variation laws of permeability of coal samples under different temperatures, confining pressures, and gas pressures were analyzed, and it was found that the permeability of coal decreased due to the existence of gas pressure and increased first and then decreased with the increase of temperature [35, 36]. Jiang et al. [37] constructed the motion equation of gas in coal under the coupling of stress field, temperature field, and sound field, which provided a new method to improve the extraction rate of coalbed methane. Some scholars divided the surrounding rock of roadway into four zones according to the change of coal permeability through numerical simulation and

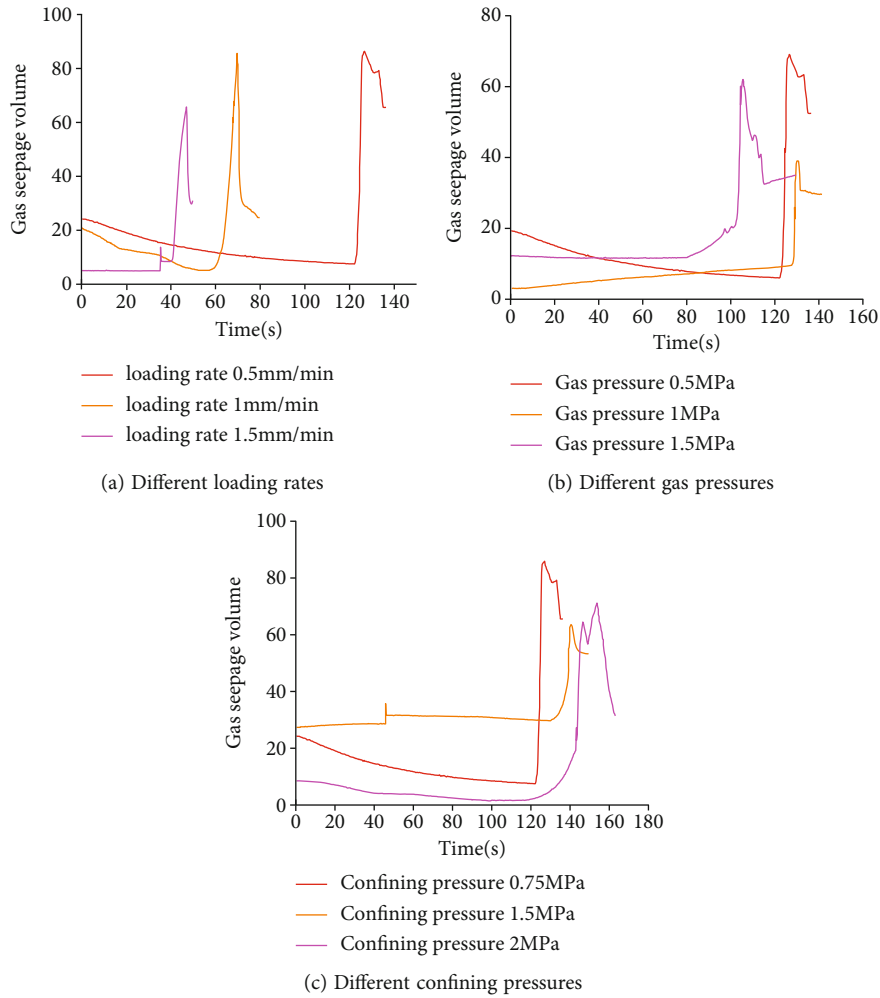


FIGURE 4: Time-gas seepage volume curve under different loading conditions.

analyzed the mechanical characteristics of different zones [38]. The change of coal permeability under different injection pressures was divided into four stages, and an overlapping method was designed to generate the permeability diagram of coal [39]. A model based on GRA-PCA-BP neural network was built to predict dynamic disasters of coal-gas compounds [40]. Monitoring the change of gas seepage rate with axial stress and confining pressure under different cyclic loading and unloading conditions, it was found that the effect of axial stress on gas seepage rate was less than that of confining pressure under the same stress state [41]. By monitoring and analyzing the change law of electric potential signal produced in the loading process of gas-bearing coal, the damage and destruction of coal were obtained [42], and the relationship between acoustic emission and gas concentration was also analyzed [43]. Jiang et al. [44] carried out fundamental research on the early warning technology of coal rock gas composite dynamic disasters and constructed a new real-time early warning platform for composite dynamic disasters. The strain of gas-bearing raw coal and coal briquette at the moment of adsorption pressure relief was analyzed, and it was found that the deformation

of raw coal had certain reversibility at the moment of pressure relief, while the coal briquette had a plastic failure [45].

Many existing studies were based on the analysis of the influence of various loading factors on the change of mechanical characteristics or gas seepage of gas-bearing coal under different loading conditions, as well as the study of their at different deformation stages. However, combined with the mechanical characteristics and permeability, there were few studies on the identification of precursor characteristics of instability failure of gas-bearing coal. This paper attempted to propose a comprehensive early warning index by combining the variation characteristics of stress and gas seepage of gas-bearing coal under three-dimensional stress loading, which was used to determine whether the specimen entered the crack propagation stage, and provided theoretical guidance for the safe mining of gas-bearing coal mines.

2. Experimental System and Scheme

2.1. Experimental System. The gas-bearing coal loading experimental system includes an axial loading system,

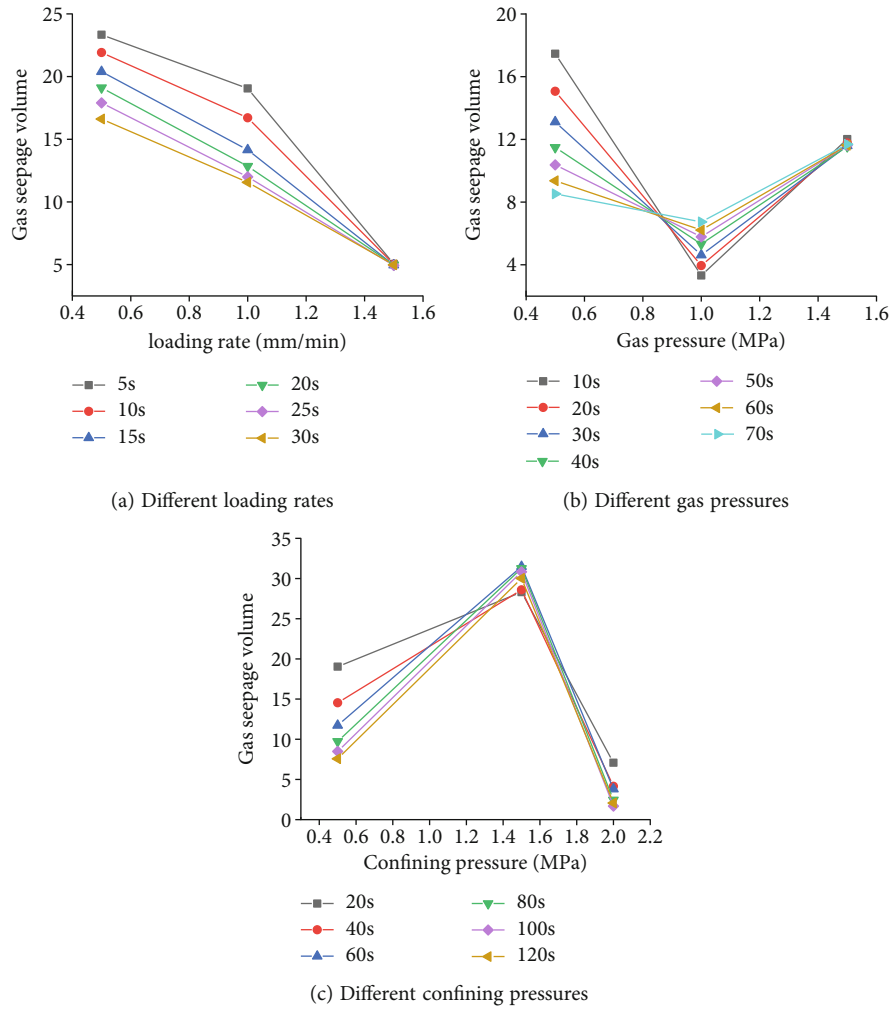


FIGURE 5: Gas seepage volume at the same time under different loading conditions.

confining pressure loading system, and gas seepage system, as shown in Figure 1. The system can realize the deformation and failure experiment of fluid-solid coupling medium under load, effectively simulate the stress environment of deep coal and rock mass, and monitor the stress, strain, and gas flow in real-time during the whole process under load. The axial loading system adopts YAW4306 mechanical testing equipment, which can realize displacement control and force control; the loading speed can be between 60 and 60000 N/s; and the accuracy is $\pm 1\%$. The confining pressure loading system replaces the traditional hydraulic oil, using nitrogen to impose confining pressure. It solves the sealing problem when the sensor data line in the cylinder is connected. The gas seepage volume data acquisition and analysis system use USB8516 data acquisition instrument and DasView2.0 analysis software.

2.2. Specimen Preparation. The coal sample processing was strictly in accordance with the national rock mechanics test standards, the sample size was $\varnothing 50 \text{ mm} \times 100 \text{ mm}$, and the upper and lower surface roughness was not more than $\pm 0.05 \text{ mm}$. In order to ensure the gas tightness, the prepared

samples were packaged by sealing ring and heat shrink tube, and the packaged sample was shown in Figure 2.

2.3. Test Procedure

- (1) The loading rates were set to 0.5 mm/min, 1 mm/min, and 1.5 mm/min; the gas pressures were set to 0.5 MPa, 1 MPa, and 1.5 MPa; and the effective confining pressures were set to 0.75 MPa, 1.5 MPa, and 2 MPa;
- (2) Connect the device and pipeline, check the air tightness of the device, put the encapsulated sample into the test chamber, seal the chamber, and vacuum for 4 hours;
- (3) Prestressed force 200 N was applied to the starting press so that the sample was fixed, and then, nitrogen was filled according to the designed confining pressure;
- (4) Open the adsorption gas intake valve, and keep the design pressure value to make the sample adsorb for 4 hours;

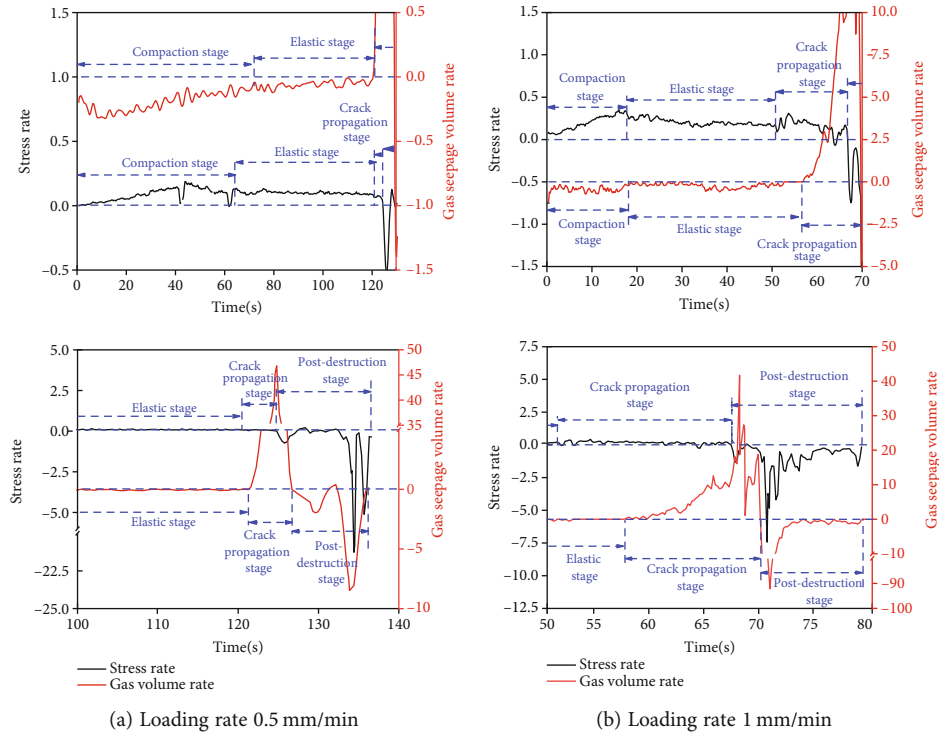


FIGURE 6: Rate curves of stress and gas seepage volume under different loading rates.

- (5) Start the press for axial loading, and open the flow-meter pipe valve to monitor gas flow.

The control variable method was used to design the test scheme, and the variables were loading rate, confining pressure, and gas pressure. The specific experimental scheme was shown in Table 1.

3. Experimental Results

3.1. Mechanical Characteristics under Different Loading Conditions. Figure 3 was based on the test results of axial stress with time under different loading conditions. It could be seen that the axial stress had a similar change rule with time under different loading conditions: increasing with

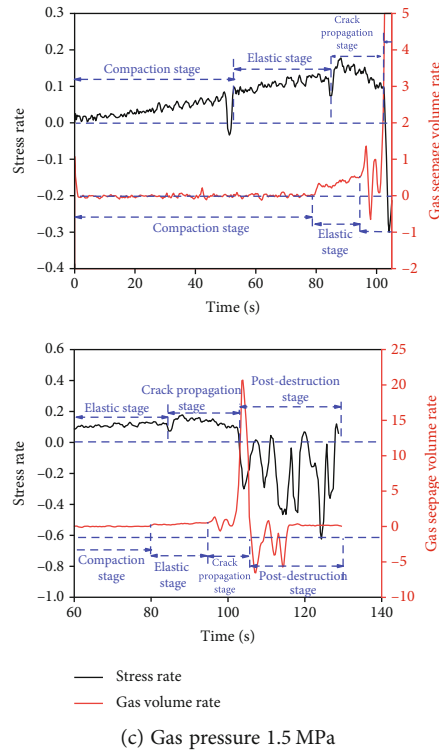
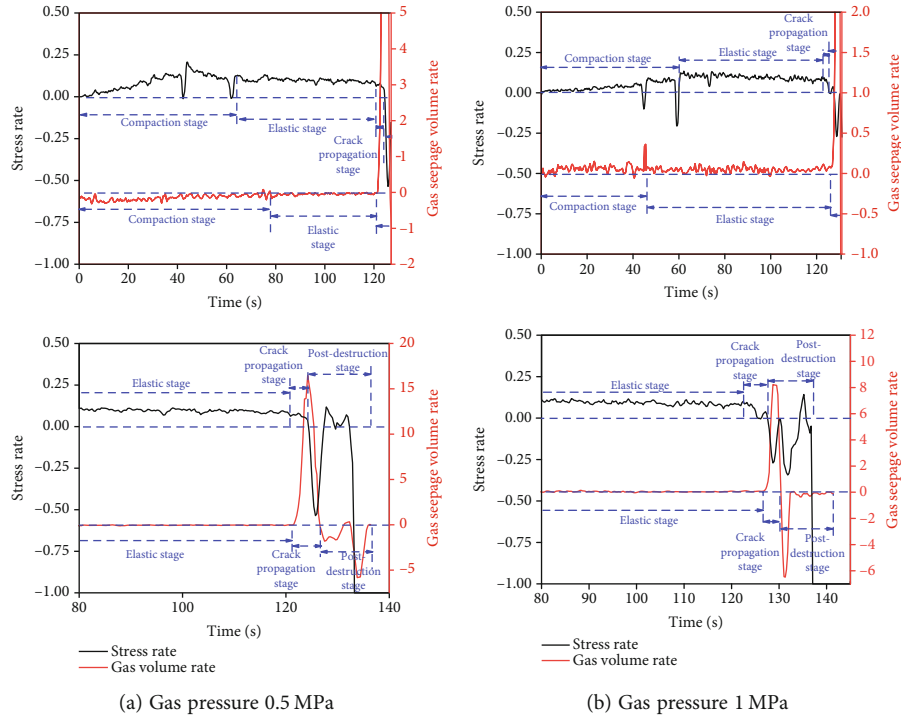


FIGURE 7: Rate curves of stress and gas seepage volume under different gas pressures.

the increase of loading time. According to the experimental results, the loading rate had a strengthening effect on the strength of coal. When the loading rate was lower, the internal cracks of coal samples had sufficient development time, resulting in an increase in deformation and a decrease in the bearing capacity of coal samples, and the peak strength was smaller. The gas was mainly stored in the coal body in

the adsorption and free states. The adsorbed gas caused the expansion deformation of the coal matrix. The adsorbed gas caused the expansion deformation of the coal matrix. The free gas had an expansion effect on the coal body, and the gas's erosion effect weakened the coal body's ability to resist the external load. Therefore, the greater the gas pressure, the smaller the strength of the sample. Due to the

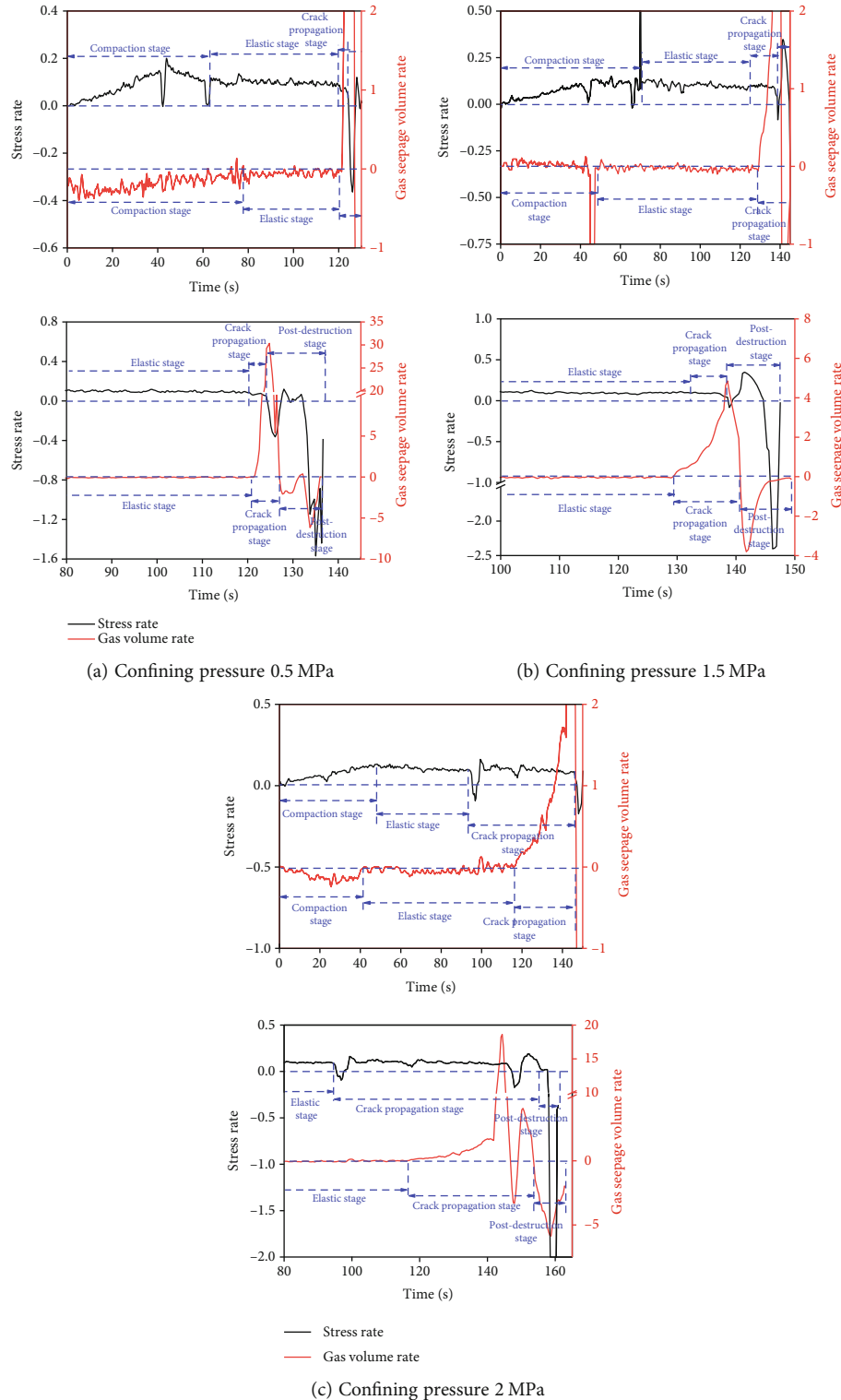


FIGURE 8: Rate curves of stress and gas seepage volume under different confining pressures.

confining pressure, the closure of pores and cracks in the coal body increased. When entering the later stage of loading, tiny pores and cracks began to merge and form macroscopic cracks, and the coal body began to expand. However, due to the existence of confining pressure, the development of pores and cracks was hindered, and the expansion effect

was constrained. With the increase of confining pressure, this constraint was more obvious, so the strength of coal was larger.

3.2. Variation Characteristics of Gas Seepage Volume under Different Loading Conditions. It could be seen that almost

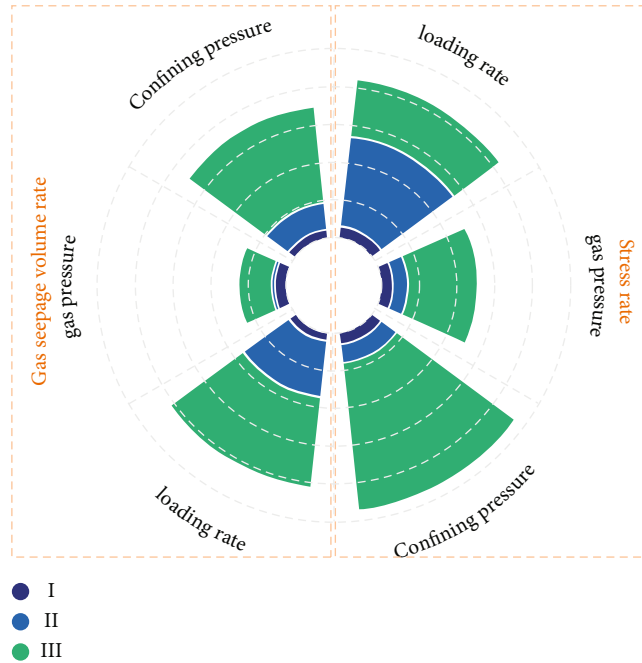


FIGURE 9: Percentage of crack propagation duration of coal under different stress states.

all the gas seepage volume decreased firstly and then increased rapidly with the increased time, as shown in Figure 4. In the early stage of loading, the internal pores of coal samples were compacted, the gas seepage ability was weakened, and the gas seepage volume was reduced. With the loading, the samples began to appear with a large number of unrecoverable deformation, the original crack propagation produced large cracks, and the volume of coal expanded, resulting in a large number of gas gushing and the gas seepage volume increasing rapidly. However, there were some special changes: the gas seepage basically remained stable during the loading process and increased rapidly in the later stage of loading, such as a loading rate of 1.5 mm/min, gas pressure of 1.5 MPa, and confining pressure of 1.5 MPa.

Before the overall failure of the specimen occurred, under the condition of constant confining pressure and gas pressure, the loading rate had a negative linear relationship with the change of gas seepage volume, in which the gas flow decreased with the increase of loading rate, as shown in Figure 5(a). The gas seepage volume of coal samples decreased first and then increased with the increase of gas pressure, in which the relationship between gas seepage volume and gas pressure conformed to the quadratic polynomial, as shown in Figure 5(b). The gas seepage volume and confining pressure show a negative quadratic polynomial relationship, as shown in Figure 5(c), and there was a critical confining pressure. When the confining pressure was less than this value, the gas seepage volume increased with the increase of confining pressure, and when it exceeded this value, the volume decreased with the increase of confining pressure.

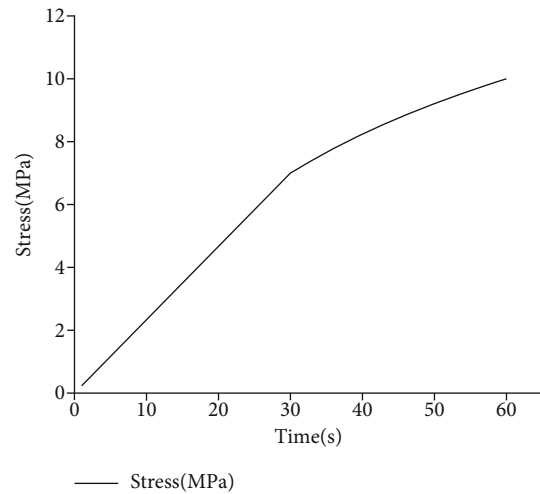


FIGURE 10: Variation curve of loading stress.

3.3. *The Variation Rate Laws of Stress and Gas Seepage Volume of Gas-Bearing Coal.* The peak stress of coal samples changed regularly with the change in loading conditions, which was consistent with the theoretical change law. However, the gas seepage volume did not necessarily change regularly, and the gas seepage volume reflected the pores and cracks of the sample. When the specimen underwent large deformation, it did not mean that the sample produced large cracks, but it might be that the original pores inside the sample were compacted or the cracks were compacted. At this time, the gas seepage volume might decrease or remain stable, so the stress mutation of the sample did not mean that

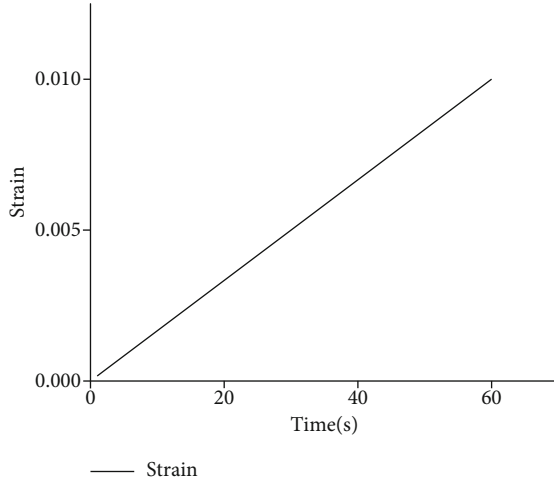


FIGURE 11: Time-strain curve diagram.

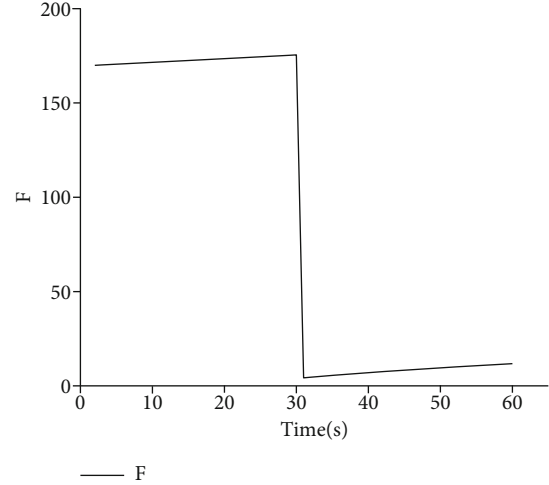
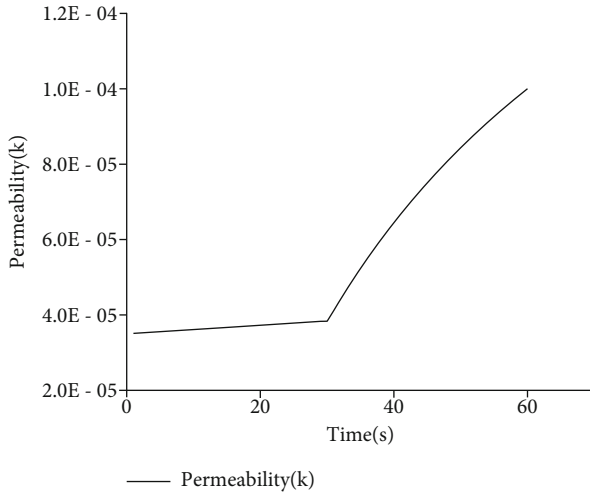
FIGURE 13: Variation curve of the F value of gas-bearing coal.

FIGURE 12: Variation curve of permeability of gas-bearing coal.

TABLE 2: Gas-bearing coal parameters.

Parameter name	Numerical value	Unit
Initial permeability (k_0)	3.5×10^{-5}	mD
Initial porosity (ϕ_0)	0.15	—
Elastic modulus (E_s)	2000	MPa
Peak stress (σ_c)	10	MPa
Yield stress (σ_s)	7	MPa
Peak permeability (k_{\max})	10×10^{-5}	mD

the gas seepage volume at this moment would also change. Therefore, the analysis of stress rate and gas seepage volume rate could more specifically reflect the deformation and damage of the sample.

According to Figures 6–8, with the increase in loading time, the deformation of the samples was also increased, the structures of the samples became denser and denser,

and the gas seepage volume was gradually reduced. The same deformation required greater stress, and the stress rate increased. Subsequently, cracks and holes in the sample were gradually compacted, and the sample entered the elastic stage, in which the stress rate remained stable, and the gas seepage rate was close to 0. When the specimen was compressed more than the elastic deformation that the specimen could withstand, the specimen entered the crack propagation stage, in which the small cracks penetrated to produce new large cracks and induced the overall instability failure of the specimen, the gas seepage volume increased rapidly, and the rate increased gradually. At this time, the solid modulus of the specimen decreased, in which the same deformation required smaller stress, and the stress rate decreased rapidly.

The ratios of crack propagation time to the total loading time of coal samples under different loading rates, gas pressures, and confining pressures were analyzed, as shown in Figure 9, and the I, II, and III symbols in the graphs represented the stress from small to large. It could be seen from the figure that with the increase of loading rate or gas pressure, the percentage of crack propagation duration almost showed an increasing trend, especially under the condition of changing confining pressure. For example, when the confining pressure was 1.5 MPa, the percentage of crack propagation duration of stress rate was 5.04% and that of gas seepage volume rate was 7.19%, and when the confining pressure was 2 MPa, the percentage of crack propagation duration of stress rate was 18.45% and that of gas seepage volume rate was 25.64%. However, the gas seepage volume rates first decreased and then increased with the increase of gas pressure, and when the gas pressure was 1 MPa, the gas seepage volume rate was the smallest, 0.79%. This might be due to the adsorption gas expansion stress being greater than the free gas pressure, resulting in less change in seepage volume. At the same time, it was also found that under the same stress state, the stress rate and gas seepage volume rate of coal samples had different proportions during the duration of crack propagation. For example, when the loading

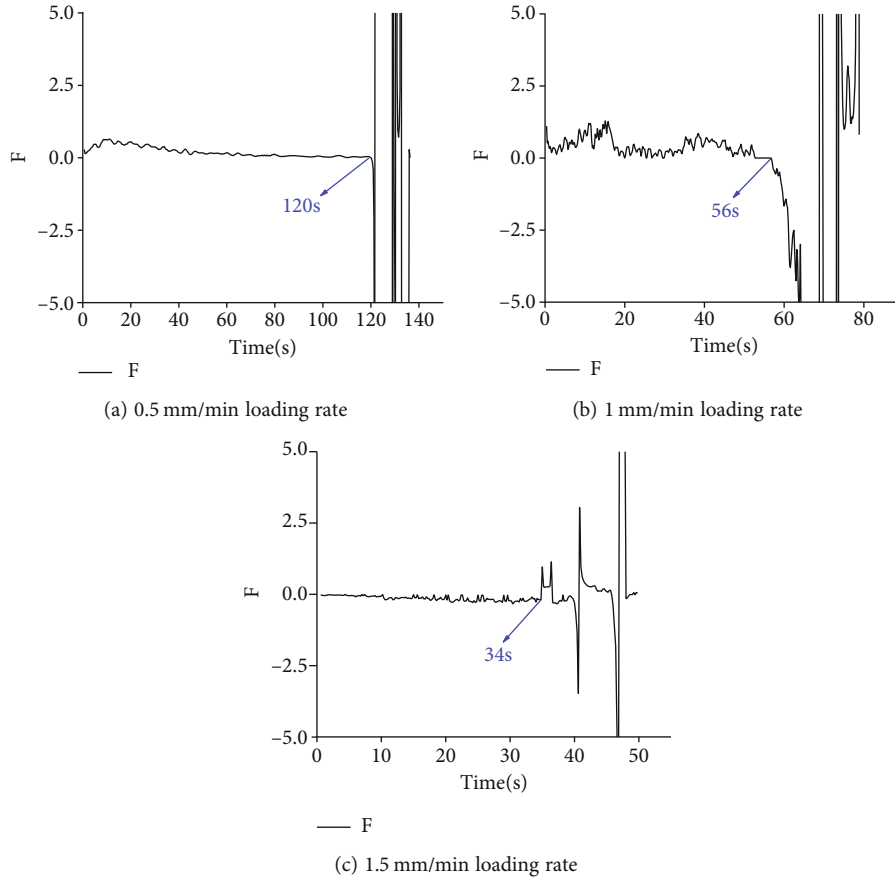


FIGURE 14: The variation curve of the F value under different loading rates.

rate was 1.5 mm/min, the percentage of crack propagation duration of stress rate was 15.22%, and that of gas seepage volume rate was 23.91%. Therefore, it could be known that under the same conditions, the time of the gas seepage volume rate and stress rate entering the crack propagation stage was different, and under different stress conditions, the response characteristics of the gas seepage volume rate and stress rate to the crack propagation stage were different. Therefore, only based on the change rule of the stress rate or the gas seepage volume rate to determine whether the specimen was in the crack propagation stage might cause the result of early warning time delay.

4. Discussion

4.1. Theoretical Model of Stress Rate–Gas Seepage Volume Rate under Triaxial Pressure. Coal is a pore medium; the presence of gas will reduce the strength of coal. According to the Terzaghi effective stress principle, the constitutive equation of gas-bearing coal is as follows:

$$\sigma^e = \sigma - \alpha p \delta_{ij}, \quad (1)$$

where σ^e is effective stress, σ is total stress (pressure is positive), α is effective stress coefficient, p is gas pressure, and δ_{ij} is Kronecker symbol ($i = j$, $\delta_{ij} = 1$; $i \neq j$, $\delta_{ij} = 0$).

Because there are two kinds of gas occurrence forms in coal, free gas mainly exists in coal cracks, which plays an expansion effect on coal, and the adsorbed gas mainly exists in the pores of the coal matrix, which has an adsorption expansion effect on coal. The expansion stress can be calculated by the following formula:

$$\sigma_{sw} = \frac{2a\rho R_0 T(1-2\nu)\ln(1+bp)}{3V_m}, \quad (2)$$

where a and b are gas adsorption constants; p is gas pressure; ν is Poisson's ratio of coal sample; ρ is density; R_0 is the molar gas constant, equal to 8.31; T is absolute temperature; and V_m is molar volume, equal to $22.4 \times 10^{-3} \text{ m}^3/\text{mol}$.

Due to the damage effect in the deformation process of gas-bearing coal, the damage variable should be considered when calculating the effective stress. Assume that under isotropic damage conditions, the calculation formula of effective stress is

$$\sigma^{e'} = \frac{\sigma - \delta_{ij}(\varphi p + ((2a\rho R_0 T(1-2\nu)\ln(1+bp))/3V_m))}{1-D}, \quad (3)$$

where φ is the equivalent porosity of coal containing gas and D is the damage variable.

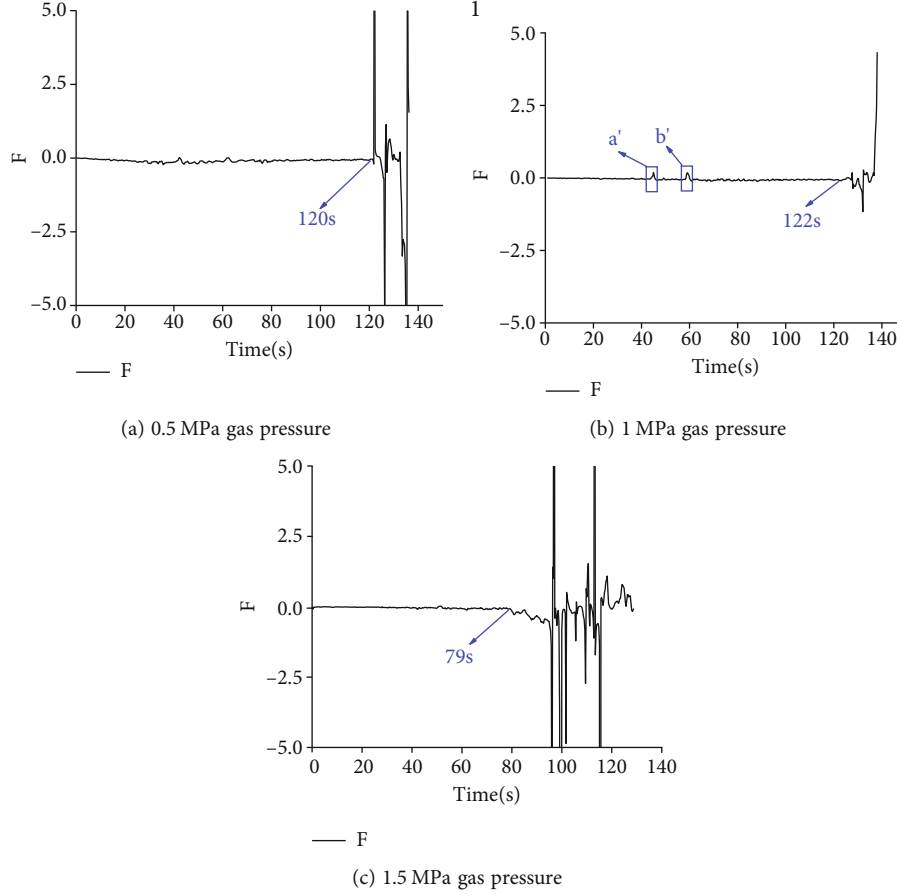


FIGURE 15: The variation curve of the F value under different gas pressures.

When the coal sample is subjected to three-dimensional stress loading, the calculation formula of axial total stress is as follows:

$$\sigma_z^{e'} = \sigma_z - \nu\sigma_x - \nu\sigma_y, \quad (4)$$

where σ_z is axial stress; σ_x and σ_y are transverse stress. And when σ_x equals σ_y , $\sigma_z^{e'} = \sigma_z - 2\nu\sigma_x$.

Then, the calculation formula of axial strain is

$$\varepsilon_z = \frac{\sigma_z - 2\nu\sigma_x - \delta_{ij}(\phi p + ((2a\rho R_0 T(1-2\nu)\ln(1+bp))/3V_m))}{(1-D)E_s}. \quad (5)$$

The formula of volume strain is

$$\varepsilon_v = \frac{\sigma_z - \sigma_x - \delta_{ij}(\phi p + ((2a\rho R_0 T(1-2\nu)\ln(1+bp))/3V_m))}{(1-D)E_s}. \quad (6)$$

The relationship between damage variable and stress can be expressed as $D = m\sigma^n$, and m and n are coal sample parameters.

According to the effective stress and the strain equivalence principle proposed by Lemaitre, stress acting on dam-

aged materials will cause strain equivalence, and the calculation formula is as follows:

$$\sigma^{e'} = E(1-D)\varepsilon. \quad (7)$$

In the crack propagation stage, the stress and strain are no longer linear, assuming that the relationship between stress and strain is as shown:

$$\sigma = 10 \log_{10}(1000\varepsilon). \quad (8)$$

With the increase of deformation, the permeability of gas-bearing coal will change. According to the Kozeny-Garman equation of seepage mechanics and the study of Wang [46], the calculation formula of permeability is as follows:

$$k = \begin{cases} k_e = \frac{k_0}{1 + \varepsilon_v} \left[1 + \frac{\varepsilon_v}{\phi_0} + \frac{(\Delta p/Ks)(1 - \phi_0)}{\phi_0} \right]^3 & \text{elastic stage,} \\ (k_{\max} - k_e) \left(\frac{\sigma^{e'} - \sigma_s}{\sigma_c - \sigma_s} \right) + k_e & \text{crack propagation stage,} \\ k_{\max} & \text{failure stage,} \end{cases} \quad (9)$$

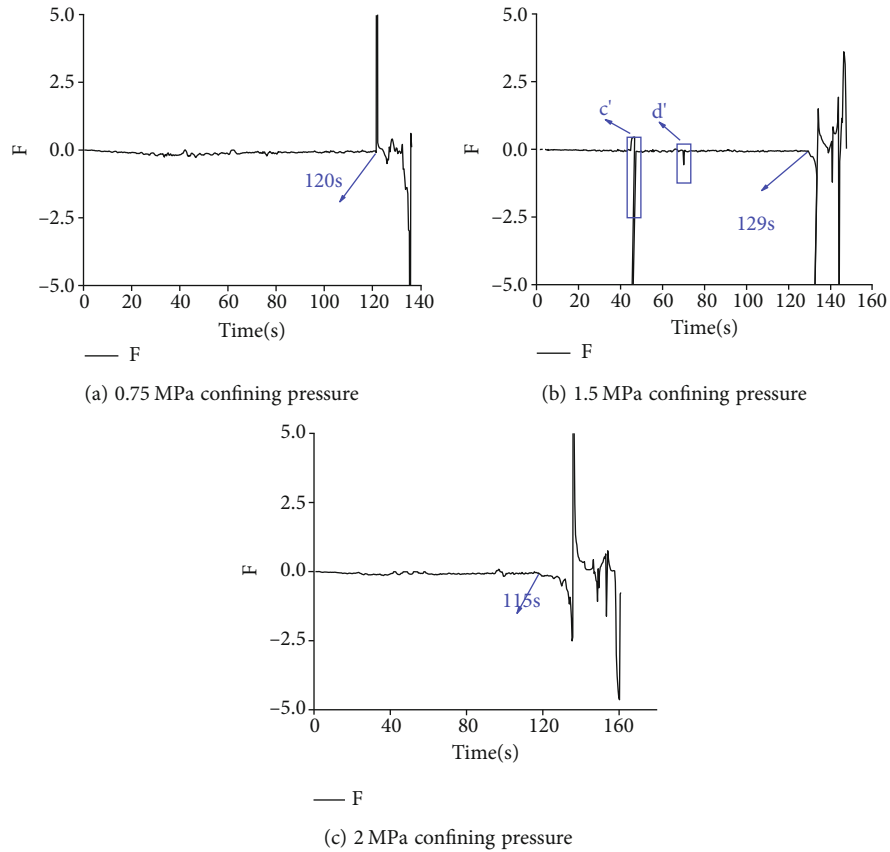


FIGURE 16: The variation curve of the F value under different confining pressures.

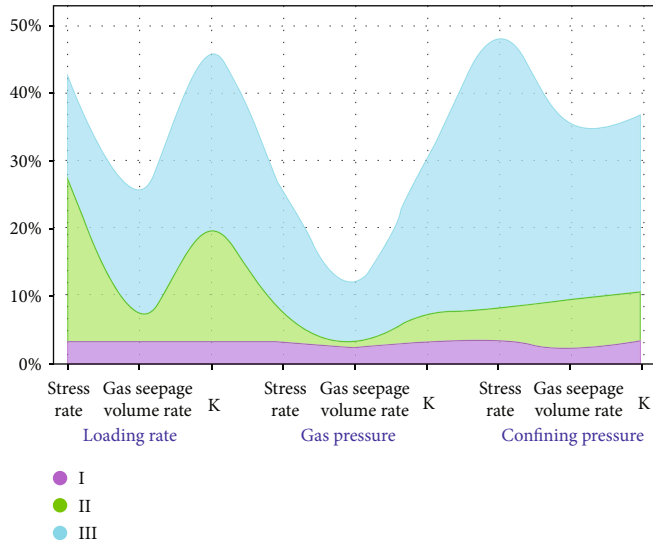


FIGURE 17: Proportional accumulation diagram of each index at the crack growth stage.

where k is the permeability of coal containing gas; k_e is the permeability in the elastic stage; k_0 is the initial permeability of coal containing gas; ε_v is the volumetric strain; ϕ_0 is the initial porosity; Δp is the Gas pressure increment; σ_s is the

yield stress intensity; σ_c is the peak stress intensity; and k_{max} is the permeability at peak stress.

It could be seen that the permeability of the sample increased with the increase of the stress of the loaded gas-

bearing coal; thus, it was considered that there was a certain internal relationship between the change of stress and gas permeability in the process of loading. Assuming that the gas-bearing coal in unit time t would generate stress $\Delta\sigma$, accompanying gas seepage volume Δk , the damage state of coal samples could be judged by the ratio of stress increment to permeability increment. Because the permeability was small, $\log_{10}(k)$ was calculated, and supposing the decision value was F , the calculation formula was as follows:

$$F = \frac{\Delta\sigma}{\Delta \log_{10}(k)}. \quad (10)$$

Since this experiment was a loading test on coal body by changing axial stress under fixed confining pressure and gas pressure, confining pressure and gas pressure were considered as fixed values. Assuming that the axial loading strain was linearly loaded with time, as shown in Figure 10, the theoretical values of stress and gas permeability of coal samples under constant gas pressure and confining pressure were calculated according to the formula; the results are shown in Figures 11 and 12, and the parameter settings of gas-bearing coal model are shown in Table 2. At the same time, the F value was calculated and its variation with the loading time was obtained, as shown in Figure 13.

It was found from the theoretical model and Figures 11 and 12 that with the increase of effective strain, stress and permeability increased gradually, in which the increasing trend gradually increased. According to Figure 13, it could be seen that the F value of gas-containing coal remained stable at the early stage of loading. With the increase in loading time, the F value began to decrease rapidly until the overall failure of the specimen occurred. Therefore, it was feasible to use the rapid decline time of the F value as the starting time for the sample to enter the crack propagation stage.

4.2. Presentation of Early Warning Index. Based on the F value, the instability early warning of loaded gas-bearing coal was studied, and the variation laws of the F value of gas-bearing coal under different loading rates, confining pressures, and gas pressures loading conditions were analyzed. The results are shown in Figures 14–16.

According to Figures 14–16, it was seen that when the specimen entered the crack propagation stage, the F value changed significantly, from a stable state to a rapid decrease. When the minor local instability occurred, the F value also had the corresponding response characteristics, such as a ' \sim ' in Figures 15 and 16, in which the F value mutated and then restored to stability. These showed that the F value had an excellent response effect on the damage state of the sample, so it was feasible and had a good early warning effect to use the F value as an early warning index of instability and failure of gas-bearing coal. The above conclusions were also well confirmed on site. In order to prevent and control coal and gas outbursts, measures such as coal seam water injection and water conservancy punching were often adopted to reduce the effective stress in coal and improve the permeability of the coal seam. When the absolute value of F was small and remained stable, it could be considered that the possibility of coal and gas outburst in the

coal seam was slight, and the risk was low. When the absolute value of F increased rapidly, it indicated that at this time, the pressure increment or the gas seepage increment was large, and it was likely that the coal body was ruptured, in which the prevention and control measures needed to be taken in time.

The ratios of the crack propagation stage to total deformation time of the coal samples under different stress states were analyzed, and the results are shown in Figure 17. The ratios of the crack propagation stage of early warning index F value were generally greater than those of stress rate and gas seepage rate, indicating that the F value had higher sensitivity and time advance characteristics for the specimen entering the crack propagation stage. Therefore, it was of great significance to use the F value as the early warning index of instability of gas-containing coal specimens.

5. Conclusions

Based on theoretical analysis and laboratory tests, the variation laws of stress rate and gas seepage volume rate with the coal deformation and damage state were studied, and the results provided an important theoretical basis for the early warning of coal and gas outburst. The main conclusions were as follows:

- (1) From the perspective of gas seepage flow and stress, the influences of adsorption gas expansion stress and gas pressure on coal strength were considered and the influences of loading rates, confining pressures, and gas pressures on coal strength were analyzed. The variation laws of stress rate and gas seepage volume rate of gas-bearing coal in different loading stages were studied, and the precursor characteristics of coal instability were revealed.
- (2) The dynamic evolution model of the stress rate and gas seepage rate of gas-bearing coal in the elastic stage and crack propagation stage under the triaxial stress state was established. The theoretical model calculated the ratio F of the two. It was found that the F value maintained low-value stability in the elastic stage. The absolute value of the F value increased rapidly when the specimen entered the crack propagation stage. Therefore, the F value was used as an early warning index to evaluate the damage state of the specimen. The experimental verification showed that the model of stress rate-gas seepage volume rate had good applicability, which could reflect the evolution trend of the damage degree of the specimens.
- (3) The variation law of early warning index F in the loading experiment of gas-containing coal was analyzed. It was found that the F value had obvious response characteristics when the specimen entered the crack propagation stage, and its response time was earlier than the stress rate or the gas seepage volume rate. Therefore, the F value was used as the early warning index of gas-containing coal instability failure, with a positive reference value for disaster warning.

Data Availability

The data used to support the findings of this study are included within the article.

Conflicts of Interest

The authors declare that they have no conflicts of interest regarding the publication of this study.

Acknowledgments

This work was supported by the Open Foundation of Key Laboratory of Safe and Effective Coal Mining (Anhui University of Science and Technology), Ministry of Education (JYBSYS2021102); the National Natural Science Foundation of China (52174218, 51774280); and the Science and Technology Planning Project of Guizhou Province, China (No. [2022] General 078). The authors gratefully acknowledge the financial support of the above-mentioned agencies.

References

- [1] H. Xie, L. Wu, and D. Zheng, "Prediction on the energy consumption and coal demand of China in 2025," *Journal of China Coal Society*, vol. 44, no. 7, pp. 1949–1960, 2019.
- [2] F. Zhou, T. Xia, X. Wang, Y. Zhang, Y. Sun, and J. Liu, "Recent developments in coal mine methane extraction and utilization in China: a review," *Journal of Natural Gas Science and Engineering*, vol. 31, pp. 437–458, 2016.
- [3] Y. Pan, "Integrated study on compound dynamic disaster of coal-gas outburst and rockburst," *Journal of China Coal Society*, vol. 1, pp. 105–112, 2016.
- [4] Q. Zhang, C. Yang, X. Li, Z. Li, and Y. Li, "Mechanism and classification of coal and gas outbursts in China," *Advances in Civil Engineering*, vol. 2021, 12 pages, 2021.
- [5] C. Gao, D. Liu, Z. Li, Y. Cai, and Y. Fang, "Fluid performance in coal reservoirs: a comprehensive review," *Geofluids*, vol. 2021, 33 pages, 2021.
- [6] Y. Liang, "Strategic thinking of simultaneous exploitation of coal and gas in deep mining," *Journal of China Coal Society*, vol. 41, pp. 1–6, 2016.
- [7] X. Li, Z. Cao, and Y. Xu, "Characteristics and trends of coal mine safety development," *Energy Sources, Part A: Recovery, Utilization, and Environmental Effects*, vol. 2021, pp. 1–19, 2021.
- [8] X. Li and B. Lin, "Status of research and analysis on coal and gas outburst mechanism," *Coal Geology & Exploration*, vol. 1, pp. 7–13, 2010.
- [9] L. Dou, K. Yang, W. Liu, X. Chi, and Z. Wen, "Mining-induced stress-fissure field evolution and the disaster-causing mechanism in the high gas working face of the deep hard strata," *Geofluids*, vol. 3, 14 pages, 2020.
- [10] X. He, L. Dou, T. Ren, J. He, and Z. Wang, "Mechanism of coal-gas dynamic disasters caused by the superposition of static and dynamic loads and its control technology," *Journal of China University of Mining and Technology*, vol. 47, pp. 48–59, 2018.
- [11] E. Wang, G. Zhang, C. Zhang, and Z. Li, "Research progress and prospect on theory and technology for coal and gas outburst control and protection in China," *Journal of China Coal Society*, vol. 47, no. 1, pp. 297–322, 2022.
- [12] T. Li, M. Cai, J. Wang, D. Li, and J. Liu, "Discussion on relativity between rockburst and gas in deep exploitation," *Journal of China Coal Society*, vol. 30, no. 5, pp. 562–567, 2005.
- [13] S. Peng, X. Song, J. Xu et al., "Experiment of factors affected to coal and gas outburst intensity based on hypothesis of comprehensive effect," *Coal science and technology*, vol. 44, no. 12, pp. 81–84, 2016.
- [14] M. Zhang, Z. Xu, Y. Pan, and Y. Zhao, "A united instability theory on coal(rock) burst and outburst," *Journal of China Coal Society*, vol. 16, pp. 48–53, 1991.
- [15] J. Guo, *Hazard assessment and monitoring technology of compound dynamic disaster in mine*, China University of Mining and Technology, 2013.
- [16] L. Zhu, Y. Pan, Z. Li, and L. Xu, "Mechanisms of rockburst and outburst compound disaster in deep mine," *Journal of China Coal Society*, vol. 43, pp. 3042–3050, 2018.
- [17] T. Mei, T. Li, G. Li, S. Xu, J. Yang, and H. Dong, "Mechanism study of coal and gas outburst induced by rockburst in "three-soft" coal seam," *Chinese Journal of Rock Mechanics and Engineering*, vol. 30, no. 6, pp. 1283–1288, 2011.
- [18] Y. Miao, X. Li, Y. Zhou et al., "A dynamic predictive permeability model in coal reservoirs: effects of shrinkage behavior caused by water desorption," *Journal of Petroleum Science and Engineering*, vol. 168, pp. 533–541, 2018.
- [19] M. Wei, C. Liu, Y. Liu et al., "Long-term effect of desorption-induced matrix shrinkage on the evolution of coal permeability during coalbed methane production," *Journal of Petroleum Science and Engineering*, vol. 208, article 109378, 2022.
- [20] M. Wei, E. Wang, and X. Liu, "Assessment of gas emission hazard associated with rockburst in coal containing methane," *Process Safety and Environmental Protection*, vol. 135, pp. 257–264, 2020.
- [21] X. Yang, Y. Xia, and X. Wang, "Investigation into the nonlinear damage model of coal containing gas," *Safety Science*, vol. 50, no. 4, pp. 927–930, 2012.
- [22] X. Yang, Y. Li, H. Guan, T. Li, and J. He, "Nonlinear damage creep model of coal or rock containing gas," *Applied Mechanics & Materials*, vol. 204–208, pp. 289–296, 2012.
- [23] X. Kong, S. Li, E. Wang et al., "Experimental and numerical investigations on dynamic mechanical responses and failure process of gas-bearing coal under impact load," *Soil Dynamics and Earthquake Engineering*, vol. 142, article 106579, 2021.
- [24] P. Ranjith, D. Jasinge, S. Choi, M. Mehic, and B. Shannon, "The effect of CO₂ saturation on mechanical properties of Australian black coal using acoustic emission," *Fuel*, vol. 89, no. 8, pp. 2110–2117, 2010.
- [25] C. Jin, S. Liu, P. Xu, and C. Guo, "Scale effect stress-strain model of coal containing gas," *Journal of the Brazilian Society of Mechanical Sciences and Engineering*, vol. 41, no. 3, 2019.
- [26] G. Xie, Z. Yin, L. Wang, Z. Hu, and C. Zhu, "Effects of gas pressure on the failure characteristics of coal," *Rock Mechanics and Rock Engineering*, vol. 50, no. 7, pp. 1711–1723, 2017.
- [27] J. Lu, G. Yin, B. Deng et al., "Permeability characteristics of layered composite coal-rock under true triaxial stress conditions," *Journal of Natural Gas Science and Engineering*, vol. 66, pp. 60–76, 2019.
- [28] G. Wang, W. Li, P. Wang, X. Yang, and S. Zhang, "Deformation and gas flow characteristics of coal-like materials under

- triaxial stress conditions,” *International Journal of Rock Mechanics and Mining Sciences*, vol. 91, pp. 72–80, 2017.
- [29] R. Peng, Y. Ju, J. Wang, H. Xie, F. Gao, and L. Ma, “Energy dissipation and release during coal failure under conventional triaxial compression,” *Rock Mechanics and Rock Engineering*, vol. 48, no. 2, pp. 509–526, 2015.
- [30] G. Yin, X. Li, J. Ru, and M. Li, “Disaster-causing mechanism of compound dynamic disaster in deep mining under static and dynamic load condition,” *Journal of China Coal Society*, vol. 42, no. 9, pp. 2316–2326, 2017.
- [31] T. Li and X. Pi, “Coupling catastrophes mechanism of low-gas in deep coal seams,” *Journal of China Coal Society*, vol. 44, no. 4, pp. 1107–1114, 2019.
- [32] C. Fan, S. Li, M. Luo, W. Du, and Z. Yang, “Coal and gas outburst dynamic system,” *International Journal of Mining and Technology*, vol. 27, pp. 49–55, 2017.
- [33] S. Peng, J. Xu, H. Yang, and D. Liu, “Experimental study on the influence mechanism of gas seepage on coal and gas outburst disaster,” *Safety Science*, vol. 50, no. 4, pp. 816–821, 2012.
- [34] F. Wang, Y. Liang, X. Li, L. Li, J. Li, and Y. Chen, “Study on the change of permeability of gas-containing coal under many factors,” *Energy Science & Engineering*, vol. 7, no. 1, pp. 194–206, 2019.
- [35] J. Zhang, Q. Guo, T. Zhu, and F. Wang, *Evolution of coal rock permeability with multiphysics coupling—taking Ping Mei No.10 mine as an example*, Journal of Xi’an University of Science and Technology, 2018.
- [36] Y. Yu, Z. Meng, C. Gao, Y. Lu, and J. Li, “Experimental investigation of pore pressure effect on coal sample permeability under different temperatures,” *Natural Resources Research*, vol. 31, no. 3, pp. 1585–1599, 2022.
- [37] Y. Jiang, X. Yang, X. Xian, L. Xiong, and J. Yi, “The infiltration equation of coal bed under the cooperation of stress field, temperature field and sound field,” *Journal of China Coal Society*, vol. 35, no. 3, pp. 434–438, 2012.
- [38] T. Yang, B. Li, and Q. Ye, “Numerical simulation research on dynamical variation of permeability of coal around roadway based on gas-solid coupling model for gassy coal,” *International Journal of Mining Science and Technology*, vol. 28, no. 6, pp. 925–932, 2018.
- [39] S. Zhang, J. Liu, M. Wei, and D. Elsworth, “Coal permeability maps under the influence of multiple coupled processes,” *International Journal of Coal Geology*, vol. 187, pp. 71–82, 2018.
- [40] K. Wang, K. Li, and F. Du, “Study on prediction of coal-gas compound dynamic disaster based on GRA-PCA-BP model,” *Geofluids*, vol. 2021, 11 pages, 2021.
- [41] F. Wang, X. Li, B. Cui, J. Hao, and P. Chen, “Study on the permeability change characteristic of gas-bearing coal under cyclic loading and unloading path,” *Geofluids*, vol. 2021, 12 pages, 2021.
- [42] Z. Li, Y. Niu, E. Wang et al., “Experimental study on electric potential response characteristics of gas-bearing coal during deformation and fracturing process,” *Processes*, vol. 7, no. 2, pp. 72–95, 2019.
- [43] J. Li, Q. Hu, M. Yu, X. Li, J. Hu, and H. Yang, “Acoustic emission monitoring technology for coal and gas outburst,” *Energy Science & Engineering*, vol. 7, no. 2, pp. 443–456, 2019.
- [44] F. Jiang, G. Yang, Q. Wei, C. Wang, X. Qu, and S. Zhu, “Study and prospect on coal mine composite dynamic disaster real-time prewarning platform,” *Journal of China Coal Society*, vol. 43, no. 2, pp. 333–339, 2018.
- [45] A. Zhou, K. Wang, J. Hu, and X. Fan, “Experimental research on the law of the deformation and damage characteristics of raw coal/briquette adsorption-instantaneous pressure relief,” *Fuel*, vol. 308, article 122062, 2022.
- [46] D. Wang, *Research on constitutive models and instability rules of gas-saturated coal*, Chongqing University, 2009.